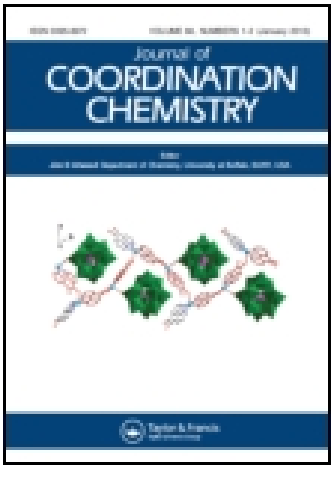

Journal of Coordination Chemistry
Publication details, including instructions for authors and subscription information:
http://www.tandfonline.com/loi/gcoo20

Synthesis, structures, and third-order nonlinear optical properties of three new copper complexes based on salicylaldehyde phenoxyacetohydrazide ligand

Caixia An[a], Xilan Feng[a], Ning Zhao[a], Ping Liu[a], Tianxi Wang[a] & Zhaoxun Lian[a]

[a] School of Chemistry and Chemical Engineering, Henan Institute of Science and Technology, Xinxiang, PR China

Accepted author version posted online: 13 Oct 2014.Published online: 07 Nov 2014.

To cite this article: Caixia An, Xilan Feng, Ning Zhao, Ping Liu, Tianxi Wang & Zhaoxun Lian (2014) Synthesis, structures, and third-order nonlinear optical properties of three new copper complexes based on salicylaldehyde phenoxyacetohydrazide ligand, Journal of Coordination Chemistry, 67:22, 3621-3632, DOI: 10.1080/00958972.2014.976212

To link to this article: http://dx.doi.org/10.1080/00958972.2014.976212

Journal of Coordination Chemistry, 2014
Vol. 67, No. 22, 3621–3632, http://dx.doi.org/10.1080/00958972.2014.976212

Synthesis, structures, and third-order nonlinear optical properties of three new copper complexes based on salicylaldehyde phenoxyacetohydrazide ligand

CAIXIA AN, XILAN FENG, NING ZHAO, PING LIU, TIANXI WANG and ZHAOXUN LIAN*

School of Chemistry and Chemical Engineering, Henan Institute of Science and Technology, Xinxiang, PR China

(*Received 22 July 2014; accepted 17 September 2014*)

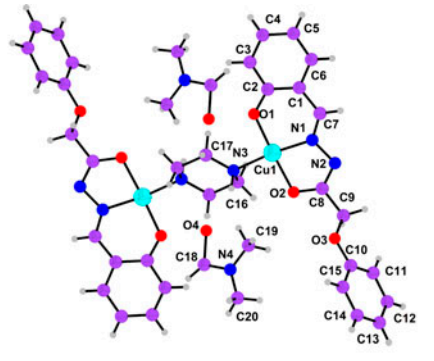

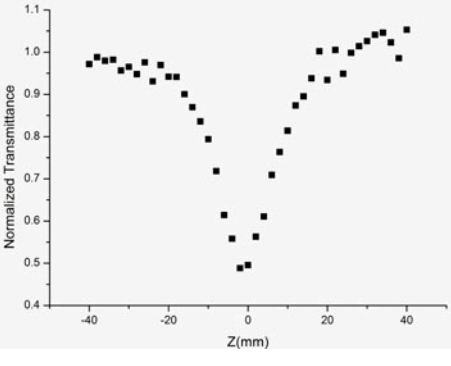

Three copper complexes have been synthesized in methanol/DMF solution at room temperature. The compounds show very strong NLO absorption properties

*Corresponding author. Email: zhaxalian@163.com

Three copper complexes, $[Cu_2(Hsa)_2(pipe)]\cdot 2DMF$ (**1**), $[Cu(Hsa)(MEA)]_n$ (**2**), and $\{[Cu_4(Hsa)_4(DMF)](DMF)\}_n$ (**3**) (pipe = piperazine; MEA = methenamine, Hsa = (2-hydroxybenzylidene)-2-phenoxyacetohydrazide), have been synthesized in methanol/DMF solution at room temperature and structurally characterized by single-crystal X-ray diffraction. In **1**, the copper(II) complexes are bridged by pipe ligands to form binuclear clusters. In **2**, the MEA ligands link copper(II) complexes to result in an infinite chain structure. Compound **3** contains tetranuclear clusters, which are bridged by Hsa to give an infinite chain structure. Third-order nonlinear optical (NLO) properties of the compounds were determined by Z-scan technique in DMF solution. All three compounds show very strong NLO absorption properties with absorptive coefficients β(MKS), 1.71×10^{-10} m W^{-1} for **1**, 1.39×10^{-10} m W^{-1} for **2**, and 9.30×10^{-11} m W^{-1} for **3**, respectively. The NLO refractive index value γ(MKS) of **3** is 5.97×10^{-18} m^2 W^{-1}. Compound **3** shows strong self-focusing behavior.

Keywords: Third-order nonlinear optics; Copper; Schiff base; Crystal structure; Z-scan

1. Introduction

The chemistry of transition metal complexes based on Schiff bases continues to be an active research field due to their potential applications in catalysis, electronics, and magnetism [1–6]. In pursuing various complexes with desired structures and properties, many types of Schiff bases have been synthesized and widely employed to construct complexes [7–17]. The tridentate ligand salicylaldehyde and its derivatives are especially interesting. These ligands coordinate metal centers through phenoxy oxygen, imine nitrogen, and deprotonated enolimine oxygen, and the complexes show interesting catalysis and magnetism. In Ni derivatives, salicylaldehyde ligands are tridentate to form mononuclear compounds, and these compounds are active catalysts in epoxidations of cis-stilbene, styrene, cyclohexene, and trans-4-octene by NaOCl under phase-transfer conditions [16]. In Cu derivatives, these compounds possess magnetic interactions covering a broad range, from antiferromagnetism to ferromagnetism [18]. Very recently, some copper(II) Schiff base compounds show excellent biological activity [7–9]. There has been interest in materials with nonlinear optical (NLO) properties due to their possible applications in optical switching, optical data processing, and optical-phase conjugation. Much of the work in this area has involved inorganic semiconductors, conjugated polymers, and organometallic compounds [19, 20]. Previous studies on Mo(W)/Cu/S clusters showed that these compounds have strong NLO absorption [21–24]. The values are 10^{-10} m W^{-1} in ~10^{-4} M dm^{-3} solution. Several groups have reported NLO properties of metal Schiff base compounds, but their work has focused on second-order NLO properties of those compounds [25–27]. It is very interesting to explore the third-order NLO properties of transition metal Schiff base complexes. In this article, we synthesized a salicylaldehyde phenoxyacetohydrazone ligand (Hsa), and three new copper complexes were obtained in the presence of secondary ligands, including piperazine and methenamine, $[Cu_2(Hsa)_2(pipe)]\cdot 2DMF$ (**1**), $[Cu(Hsa)(MEA)]_n$ (**2**), and $\{[Cu_4(Hsa)_4(DMF)](DMF)\}_n$ (**3**) (pipe = piperazine; MEA = methenamine, Hsa = (2-hydroxybenzylidene)-2-phenoxyacetohydrazide). The third-order NLO refraction and absorption of these compounds were obtained by standard Z-scan method. The third-order NLO absorptive coefficients β(MKS) are 1.71×10^{-10} m W^{-1} for **1**, 1.39×10^{-10} m W^{-1} for **2**, and 9.30×10^{-11} m W^{-1} for **3**, respectively. The NLO refractive index value γ(MKS) of **3** is 5.97×10^{-18} m^2 W^{-1}. These values are comparable to those of Mo/S/M (M = Cu, Ag) clusters and better than those of organometallic compounds, semiconductors, and fullerene [25–27].

2. Experimental

2.1. *General*

All materials were commercially available and used as received. Elemental analyses were carried out with an Elementar Vario EL III instrument. FTIR spectra were recorded from 400 to 4000 cm^{-1} on a Nicolet Magna 750 FTIR spectrometer with KBr pellets.

2.2. *Synthesis of [Cu_2(Hsa)$_2$(pipe)]·2DMF (1)*

A mixture of $Cu(CH_3COO)_2·4H_2O$ (0.3 mM, 0.075 g), Hsa (0.3 mM, 0.080 g), and pipe (0.6 mM, 0.06 g) in methanol and DMF (20 mL, V : V = 10 : 2) was stirred for 1 h and then was filtered. After slow evaporation of the mother liquor for several days, green block-like crystals suitable for X-ray diffraction were collected by hand and dried in air at ambient temperature [yield: 76% based on Cu]. $[Cu_2(Hsa)_2(pipe)]·2DMF$ **1**. Elemental Anal. Calcd for **1** (%): C, 53.62; N, 12.51; H, 5.40. Found: C, 53.63; N, 12.55; H, 5.37. IR(KBr, cm^{-1}): 3423(m), 3249(m), 3041(w), 1668(s), 1616(s), 1600(s), 1535(m), 1494(m), 1448(m), 1384 (m), 1344(m), 1203(w), 1149(m), 1089(w), 1062(w), 908(w), 754(w), 690(w), 657(m).

2.3. *Synthesis of [Cu(Hsa)(MEA)]$_n$ (2) and {[Cu_4(Hsa)$_4$(DMF)](DMF)}$_n$ (3)*

The syntheses of **2** and **3** were similar to the above description for **1** except that pipe ligands were replaced by MEA for **2**. $[Cu(Hsa)(MEA)]_n$ **2**, yield: 51% based on Cu. Elemental Anal. Calcd for **2** (%): C, 53.67; N, 17.88; H, 4.72. Found: C, 53.64; N, 17.83; H, 4.69. IR(KBr, cm^{-1}): 3455(m), 3243(m), 2944(s), 1610(s), 1542(s), 1496(s), 1448(s), 1340 (s), 1297(m), 1251(m), 1234(m), 1189(m, 1151(w), 1052(m), 1027(m), 910(s), 860(w), 906 (m), 825(s), 781(w), 748(w), 676(w). $\{[Cu_4(Hsa)_4DMF](DMF)\}_n$ **3**, yield: 87% based on Cu. Elemental Anal. Calcd for **3** (%): C, 53.80; N, 9.51; H, 4.24. Found: C, 5376; N, 9.48;

Table 1. Crystallographic data for **1–3**.

	1	**2**	**3**
Formula	$C_{40}H_{48}N_8O_8Cu_2$	$C_{21}H_{22}N_6O_3Cu_1$	$C_{66}H_{62}N_{10}O_{14}Cu_4$
M_r	859.94	469.99	1473.42
$T(K)$	298	298	293
Crystal system	Triclinic	Monoclinic	Triclinic
Space group	*P-1*	*P21/C*	*P-1*
a (Å)	10.0519(11)	11.1786(8)	14.1938(8)
b (Å)	10.6162(12)	18.2807(13)	15.3033(8)
c (Å)	11.1396(12)	10.1395(7)	17.2213(9)
α (°)	66.865(2)	90.00	108.1420(10)
β (°)	76.027(2)	98.6410(10)	104.8420(10)
γ (°)	81.850(2)	90.00	103.2210(10)
V (Å^3)	1059.3(2)	2048.5(3)	3236.6(3)
Z	1	4	2
D_{Calcd} (g/cm^3)	1.404	1.524	1.512
F (0 0 0)	466	972	1512
Reflections collected	13,355	13,331	40,910
Goodness-of-fit on F^2	0.998	1.032	1.010
$R_1[I > 2\sigma(I)]$	0.0582	0.0344	0.0465
$wR_2[I > 2\sigma(I)]$	0.1715	0.0956	0.1222
Peak/hole (e Å^{-3})	1.288/−1.053	0.744/−0.251	0.627/−0.514

Table 2. Selected bond lengths (Å) and angles (°) for **1**–**3**.

Compound **1**					
Cu(1)–O(1)	1.891(3)	Cu(1)–N(1)	1.918(3)	Cu(1)–O(2)	1.942(3)
Cu(1)–N(3)	2.003(3)				
O(1)–Cu(1)–N(1)	93.26(1)	O(1)–Cu(1)–O(2)	172.51(1)	N(1)–Cu(1)–N(3)	172.91(1)
N(1)–Cu(1)–O(2)	81.68(1)	O(1)–Cu(1)–N(3)	93.61(1)	O(2)–Cu(1)–N(3)	91.65(1)
Compound **2**					
Cu(1)–O(1)	1.8957(1)	Cu(1)–N(1)	1.9447(2)	Cu(1)–O(3)	1.9466(1)
Cu(1)–N(5)a	2.4245(2)	Cu(1)–N(3)	2.0879(2)		
O(1)–Cu(1)–N(1)	93.57(7)	N(1)–Cu(1)–O(3)	80.90(7)	O(1)–Cu(1)–O(3)	173.28(7)
O(1)–Cu(1)–N(3)	89.72(6)	N(1)–Cu(1)–N(3)	153.22(7)	O(3)–Cu(1)–N(3)	93.52(6)
O(1)–Cu(1)–N(5)a	94.03(7)	N(1)–Cu(1)–N(5)a	101.82(7)	O(3)–Cu(1)–N(5)a	90.86(6)
Compound **3**					
Cu(1)–O(1)	1.890(3)	Cu(1)–N(1)	1.929(3)	Cu(1)–N(4)	1.989(3)
Cu(1)–O(2)	1.995(3)	Cu(1)–O(6)	2.418(3)	Cu(2)–O(4)	1.904(3)
Cu(2)–N(3)	1.927(3)	Cu(2)–O(5)	1.981(3)	Cu(2)–N(6)	2.013(3)
Cu(3)–O(7)	1.900(3)	Cu(3)–N(5)	1.935(3)	Cu(3)–O(8)	1.958(3)
Cu(3)–N(8)	1.988(3)	Cu(4)–O(1)	1.882(3)	Cu(4)–N(7)	1.925(3)
Cu(4)–O(11)	1.945(3)	Cu(4)–N(2)b	1.990(3)	O(1)–Cu(1)–O(6)	96.29(1)
O(1)–Cu(1)–N(1)	92.68(1)	O(1)–Cu(1)–N(4)	92.02(1)	N(1)–Cu(1)–O(6)	114.31(1)
N(1)–Cu(1)–N(4)	171.53(1)	N(1)–Cu(1)–O(2)	80.38(1)	N(4)–Cu(1)–O(6)	72.12(1)
O(1)–Cu(1)–O(2)	172.11(1)	N(4)–Cu(1)–O(2)	95.34(1)	O(2)–Cu(1)–O(6)	83.30(1)
O(7)–Cu(3)–O(8)	170.41(1)	O(4)–Cu(2)–N(6)	90.48(1)	O(4)–Cu(2)–N(3)	93.73(1)
N(5)–Cu(3)–O(8)	81.30(1)	N(3)–Cu(2)–N(6)	166.21(1)	O(4)–Cu(2)–O(5)	174.38(1)
O(7)–Cu(3)–N(8)	91.07(1)	O(5)–Cu(2)–N(6)	95.08(1)	O(10)–Cu(4)–N(2)	81.17(1)
N(5)–Cu(3)–N(8)	174.72(1)	O(7)–Cu(3)–N(5)	93.12(1)	O(8)–Cu(3)–N(8)	94.98(1)
N(3)–Cu(2)–O(5)	80.67(1)	N(7)–Cu(4)–O(11)	91.97(1)	O(10)–Cu(4)–N(7)	94.21(1)

Note: Symmetry codes: (a) x ,− y + 1/2, z + 1/2; (b) x + 1, y + 1, z.

H, 4.22. IR(KBr, cm^{-1}): 3423(m), 3058(w), 2931(w), 1668(s), 1616(s), 1609(s), 1535(s), 1494(s), 1448(s), 1382(m), 1344(m), 1201(m), 1149(s), 1089(m), 1064(m), 908(s), 754(m), 690(w).

2.4. *Crystal structure determinations*

The X-ray intensity data for the compounds were recorded on a Bruker Smart CCD using Mo Kα radiation and a graphite monochromator at room temperature. The diffraction data were integrated using the SAINT program. Semi-empirical absorption corrections were applied using SADABS. All heavy atoms were found by direct methods with SHELX-97 [28]; other non-hydrogen atoms were found by difference Fourier synthesis. All non-hydrogen atoms were refined with anisotropic displacement parameters by full-matrix least-squares refinement. Hydrogens bound to carbons were placed geometrically and held in the rigid mode. Further details of the structure analysis are given in table 1. Selected bond lengths and angles are presented in table 2.

2.5. *NLO measurements*

The measurements of NLO properties of **1**, **2**, and **3** were carried out in DMF solution with a 1-mm quartz cell. The NLO refraction and absorption were obtained by standard Z-scan method with linearly polarized 7 ns pulses at 532 nm generated from a frequency-doubled

Q-switched Nd : YAG laser. The spatial profiles of the optical pulses were nearly Gaussian after passing through a filter. The pulsed laser was focused onto the sample cell with a 30 cm focal length mirror. Incident and transmitted pulsed energies were measured simultaneously by two energy detectors (RJP-765 Energy probes, laser precision, Laserprobe Corp.), which were linked to a computer through an RS232 interface. The sample was mounted on a translation stage that was controlled by the computer to move along the z-axis with respect to the focal point. An aperture of 0.5 mm radius was placed in front of the transmission detector. The transmittance was recorded as a function of the sample position on the z-axis (closed aperture Z-scan). For measuring the NLO absorption, the Z-dependent sample transmittance was taken without the aperture (open aperture Z-scan). In our experiments, we performed a Z-scan on the solvent (DMF) at the pulse energy focused on our samples, and no obvious NLO phenomenon was observed.

3. Results and discussion

3.1. *Crystal structure*

Selected bond distances and angles for **1–3** are listed in table 2. Single-crystal X-ray structural analysis shows that **1** is a binuclear complex, as shown in figure 1(a). The asymmetric unit of **1** consists of one Hsa ligand, one Cu(II), a part of pipe, and one DMF. The metal center is square planar, coordinated with a dinegative tridentate Hsa ligand through the deprotonated phenolic O1, azomethine N1, and deprotonated enolimide O2, and a pipe ligand with chair geometry through N3. The bond distances of Cu–O and Cu–N are 1.891 (3) and 2.003(3) Å, respectively, which are comparable to those reported in other copper complexes [17]. The C8–O2 and C8–N2 bond distances are 1.288(4) and 1.302(5) Å, respectively, suggesting that Hsa takes the enolate form of the amide functionality. The N1–C7 bond at 1.287(5) Å has a double-bond character. In **1**, two square planar copper(II) complexes are linked by pipe to result in a dimer. The separation between the symmetry-related Cu(II) ions within the dimer thus formed is 6.78(3) Å. In comparable structures [18], the metal complexes are linked by piperazine or 4,4′-bipyridine to generate a dimer. Interestingly, in these compounds, the shorter linker piperazine, in the chair conformation, is a good magnetic bridge, but the longer 4,4′-bipyridine does not act as a good magnetic bridge. In **1**, adjacent dimers are assembled into infinite chains via C–H···π interaction with $d = 3.78$ Å, as shown in figure 1(b).

As shown in figure 2(a), there are copper(II), one Hsa, and one MEA in the asymmetric unit of **2**. The copper(II) adopts a distorted square-pyramidal geometry by coordinating to one imine-N, amide-O and phenolate-O from Hsa, and two nitrogens from two distinct MEA ligands. Two oxygens and one imine-N and one nitrogen from MEA constitute the base of the square pyramid, while N5(x, $0.5 - y$, $0.5 + z$) occupies the apical position. The Cu–O and Cu–N bond lengths are comparable to those reported in other copper complexes [18], but the Cu–N5 distance is 2.4245(2) Å, which is much longer than other Cu–N bond distances. In **2**, the copper complexes are bridged by MEA to form an infinite chain along the c axis, as shown in figure 2(b). The separation between the symmetry-related Cu(II) ions within the chain thus formed is 6.14(5) Å. Interestingly, if pyridines are employed instead of MEA, binuclear copper complexes are obtained [29].

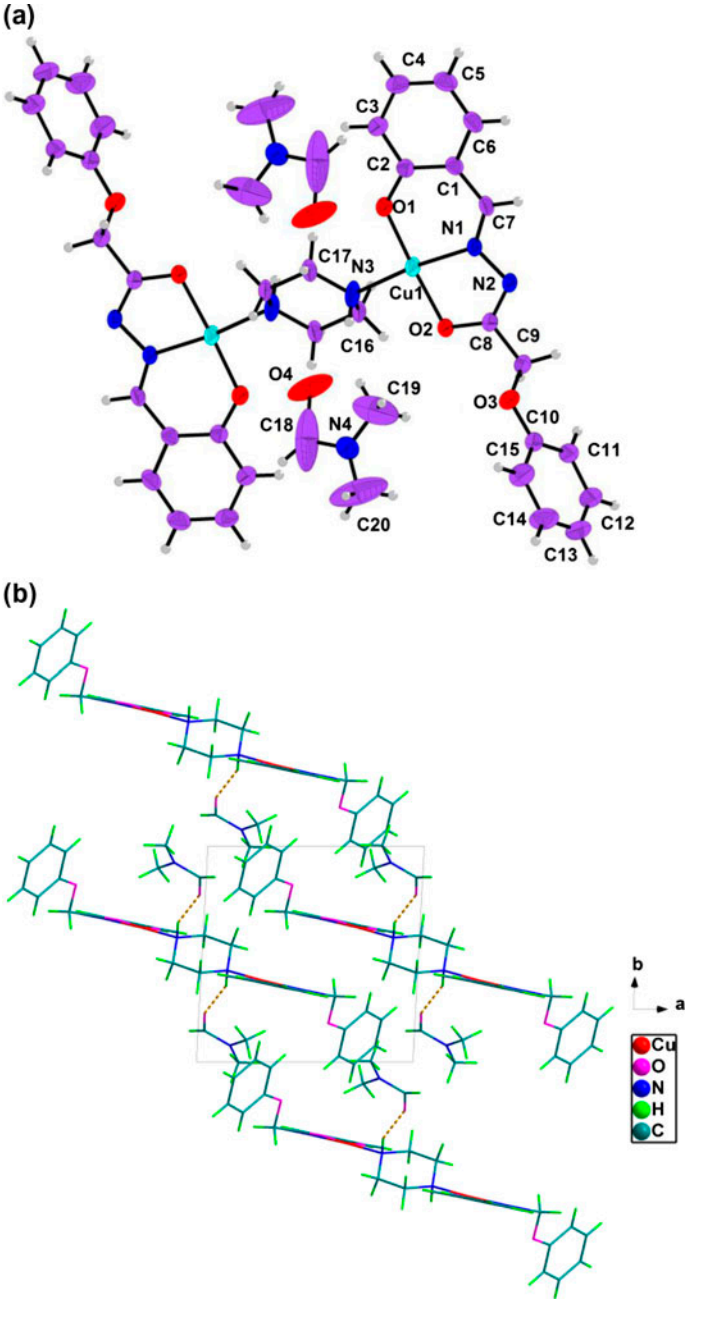

Figure 1. (a) ORTEP drawing of **1** with 50% probability displacement ellipsoids. (b) View of the 2-D extended layers of **1** down the *c* axis.

As illustrated in figure 3(a), the structure of **3** features an infinite chain. There are four independent copper(II) ions in the asymmetric unit. Cu1, Cu3, and Cu4 are in square pyramidal geometry and each is coordinated by one imine-N, amide-O, amide-N, and

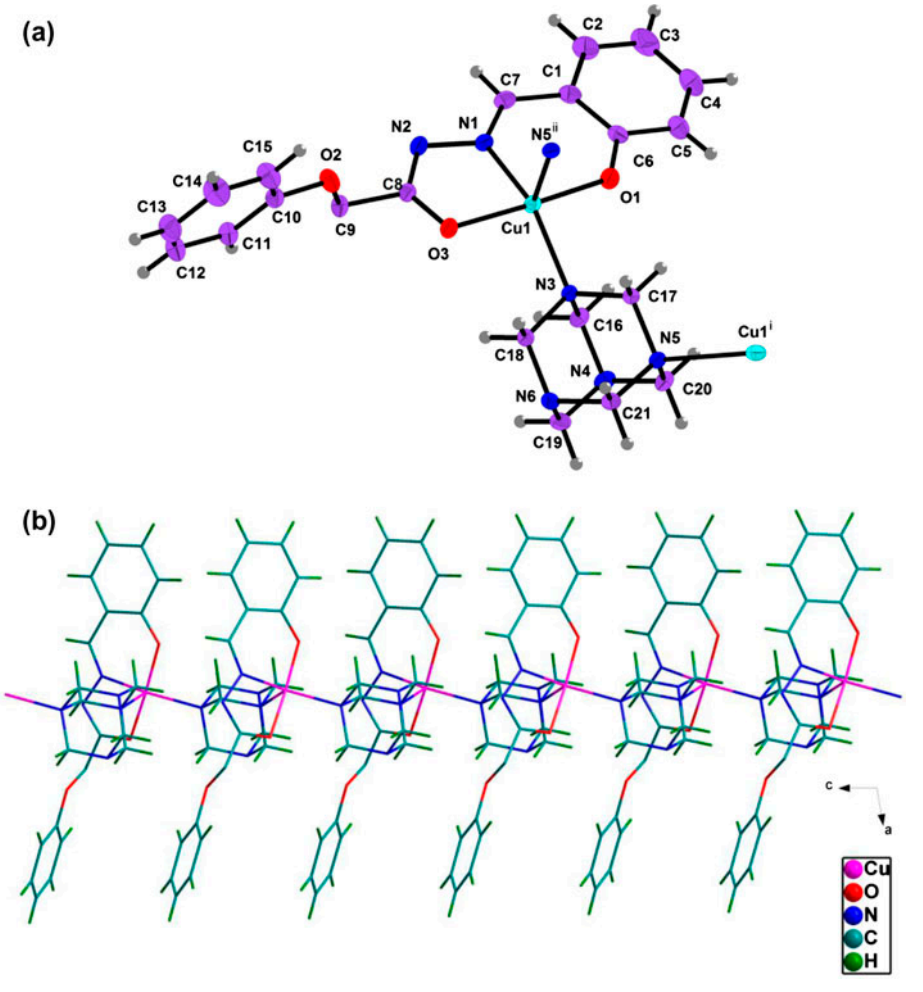

Figure 2. (a) ORTEP drawing of **2** with 50% probability displacement ellipsoids. Symmetry codes: (i) x, $0.5 - y$, $-0.5 + z$; (ii) x, $0.5 - y$, $0.5 + z$. (b) View of the 1-D chain of **2** along the b axis.

phenolate-O as the base of the square pyramid, and one ether-O occupies the apical position. Cu2 has a distorted octahedral environment and is coordinated by imine-N, amide-O, amide-N and phenolate-O as the basal plane, and one ether-O and amide-O from DMF occupy the apical positions. The Cu–O_{basal} and Cu–N bond distances are comparable to those in **1** and **2** and other copper(II) complexes [18]. The Cu–O_{apical} bond length is much longer than those of Cu–O_{basal}. In **2**, there are four unique Hsa ligands. Each Hsa is pentadentate. It chelates tridentate with a copper(II) ion through amide-O, amide-N, and phenolate-O, and bidentate chelates with adjacent copper(II) ions through imine-N and ether-O. The interconnection of the four copper(II) ions by four Hsa ligands results in an infinite chain containing tetranuclear clusters, as shown in figure 3(b). In most cases, salicylaldehyde phenoxyacetohydrazone and its derivatives are tridentate to form mononuclear or dinuclear

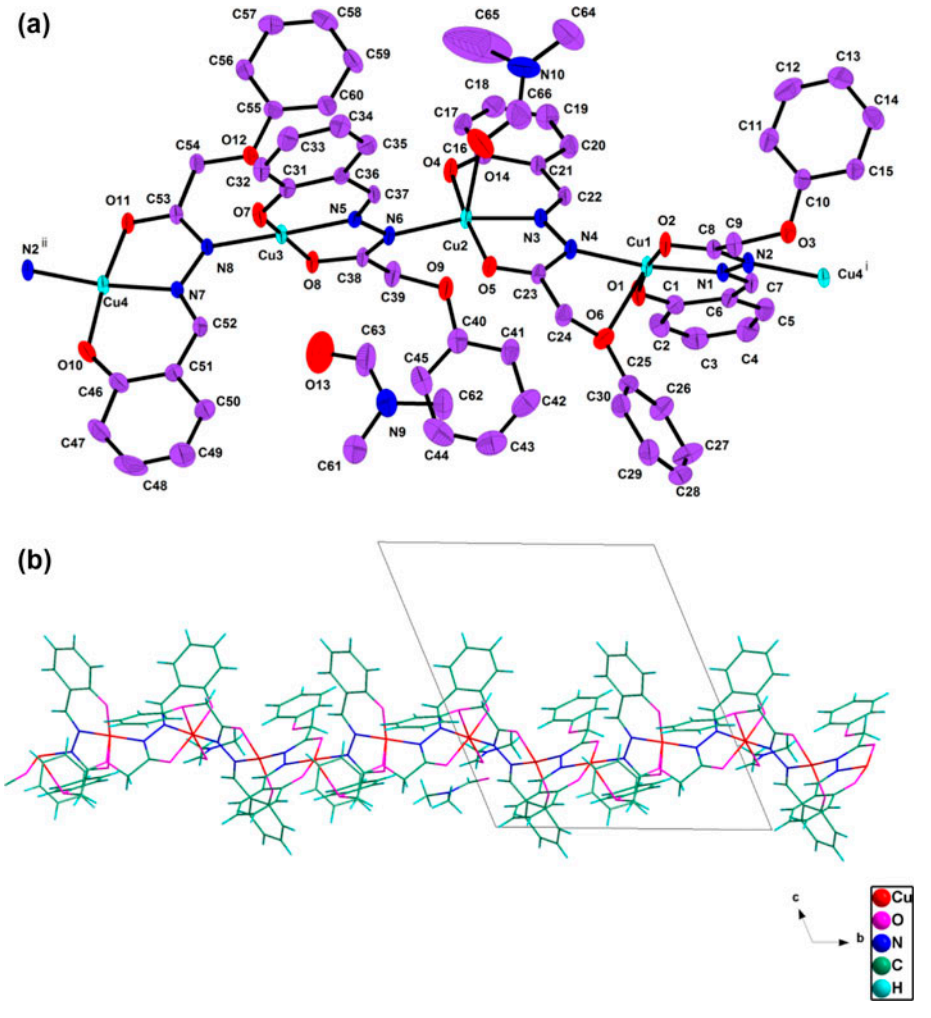

Figure 3. (a) ORTEP drawing of **3** with 50% probability displacement ellipsoids. Hydrogens are omitted for clarity. Symmetry codes: (i) $-1 + x, -1 + y, z$; (ii) $1 + x, 1 + y, z$. (b) View of the 1-D chain of **3** along the *a* axis.

compounds [30, 31]. In comparable structures, the salicylaldehyde acylhydrazones serving as tetradentate ligands were reported only in the discrete tirnuclear metal complexes of special compartmental ligands [6, 32]. The salicylaldehyde acylhydrazone acting as a tetradentate ligand coordinating to two metal ions to form infinite metal organic coordination chains is scarce, only one example is observed in the literature [12].

3.2. *Effect of the secondary ligands*

Secondary ligands play a crucial role in determining the molecular structures of **1–3**. In this study, Hsa ligands react with copper(II) to result in an infinite chain structure containing linear tetranuclear clusters; when pipe is used in the self-assembly process, binuclear complex

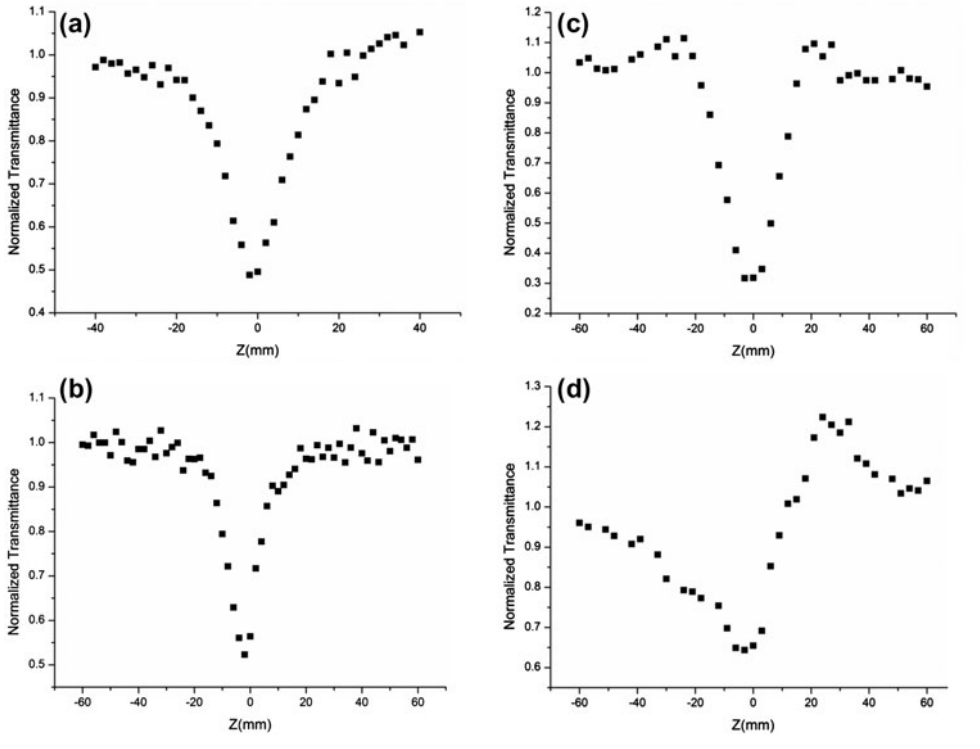

Figure 4. (a) The NLO absorptive behavior of **1**. (b) The NLO absorptive behavior of **2**. (c) The NLO absorptive behavior of **3**. (d) The NLO refractive behavior of **3**.

is obtained; if MEA is used instead of pipe, we obtained a 1-D structure complex. Other N-containing auxiliary ligands such as 2,2′-bipyridine, phenanthroline, 4,4′-bipyridine, and ethanediamine have been employed in our work, but uncharacterized blue precipitates were obtained. We also used $Cu(NO_3)_2$ and $CuCl_2$ instead of $Cu(CH_3COO)_2$, and **1–3** were isolated. The results here reported reveal that the structural diversity of the metal complexes can be adjusted by the judicious choice of auxiliary ligands.

3.3. *NLO properties*

The NLO properties of **1–3** are investigated with a 532 nm laser pulse of 7 ns in 2.5×10^{-3} M dm^{-3} for **1**, 1.9×10^{-4} M dm^{-3} for **2**, and 3.0×10^{-4} M dm^{-3} for **3** in DMF solution. These compounds show strong NLO absorption and **3** shows strong NLO refractive properties. The NLO absorption components were evaluated by *Z*-scan experiment under an open-aperture configuration. The NLO absorption data can be represented by equations (1) and (2) [33, 34],

$$T(z) = \frac{1}{\sqrt{\pi} q(z)} \int_{-\infty}^{\infty} \ln[1 + q(z)] e^{x^2} d\tau \tag{1}$$

$$q(z) = \beta I(z)\frac{1 - e^{-\alpha_0 L}}{\alpha_0} \tag{2}$$

which describe a third-order NLO process, where $T(z)$ represents the transmittance, defined as the ratio of the transmitted pulse energy and incident pulse energy. The parameters α_0 and β are the linear and nonlinear absorption coefficients, respectively. L is the sample thickness. $I(z)$ is the incident light irradiance and τ is pulse length. Figure 4(a–c) depict the NLO absorptive properties of **1–3**. It can be seen from figure 4(a–c), the normalized transmittance drops to about 0.46 for **1**, 0.51 for **2**, and 0.30 for **3** at the focus, which shows that **1–3** have strong NLO absorptive effect. The third-order NLO absorptive coefficients β(MKS) are 1.71×10^{-10} m W^{-1} for **1**, 1.39×10^{-10} m W^{-1} for **2**, and 9.30×10^{-11} m W^{-1} for **3**, respectively. These values can be comparable to those of cluster compounds [($MoOS_3Cu_3$(SCN)(py)$_5$] ($\beta = 4.8 \times 10^{-10}$ m W^{-1}) [21], [$MoCu_2OS_3$(pph)$_3$] ($\beta = 2.6 \times 10^{-10}$ m W^{-1}) [22], [Et_4]$_3$[WOS_3(CuI)$_3$(μ_2-I] ($\beta = 1.0 \times 10^{-10}$ m W^{-1}) [35], [WOS_3Cu_2(4-BuPy)$_2$]$_2$ ($\beta = 2.5 \times 10^{-10}$ m W^{-1}) [36] and [C_5Me_5)$_2Mo_2$(μ_3-S)$_3SCu_2$X(μ-X)]$_2$ (X = Cl$^-$, Br$^-$, SCN$^-$) ($\beta = 8.77 \times 10^{-10}$ m W^{-1}, 6.10×10^{-10} m W^{-1}, 7.49×10^{-10} m W^{-1}) [37].

The NLO refractive effect of **3** is estimated by dividing the normalized Z-scan data obtained under the closed-aperture configuration by the normalized Z-scan data obtained under the open-aperture configuration. An effective third-order nonlinear refractive index γ(MSK) can be derived from the difference between normalized transmittance values at valley and peak positions using equation (3),

$$\gamma(\mathrm{MKS}) = \frac{\Delta T_{\mathrm{P-V}}}{0.406\kappa L_{eff} I} \tag{3}$$

where I is the peak irradiation intensity at the focus; L is the effective optical path length; λ is the wavelength of the laser; κ is $2\pi/\lambda$. γ is the effective third-order nonlinear refractive index; and $\Delta T_{\mathrm{P\text{-}V}}$ is the difference between normalized transmittance values at the valley and peak positions. Figure 4(d) illustrates the NLO refractive properties of **3**. The data show that **3** has a positive sign for the refractive nonlinearity, which gives rise to self-focusing behavior. $\Delta T_{\mathrm{P\text{-}V}}$ is 0.61. The refractive index γ can be calculated to be 5.97×10^{-18} m^2 W^{-1}, which is comparable to that of [WCu_2OS_3(PPh$_3$)$_4$] [22].

The third-order NLO susceptibility $\chi^{(3)}$ values of **1–3** are calculated by equation (4),

$$|\chi^{(3)}| = \sqrt{\left(\frac{n_0^2 c\gamma}{80\pi^2}\right)^2 + \left(\frac{n_0^2 c\lambda\beta}{160\pi^2}\right)^2} \tag{4}$$

where c is the speed of light in a vacuum and n_0 is the linear refractive index of the sample. The $\chi^{(3)}$ values of **1–3** are 3.42×10^{-11}, 2.78×10^{-11}, and 1.91×10^{-11} esu, respectively. The corresponding modulus of the hyperpolarizability γ' can be obtained from $|\gamma'| = \chi^{(3)}/(NF^4)$, where N is the number density of a compound and $F^4 = 3$ is the local field correction factor. The $|\gamma'|$ values of **1–3** are 7.6×10^{-30}, 8.2×10^{-29}, and 3.52×10^{-29} esu. These values are comparable to those of [(n-Bu)$_4$ N]$_2$[$MoOS_3$(CuSCN)$_3$] ($\gamma' = 4.8 \times 10^{-29}$ esu) [38], [WOS_3Cu_2(PPh$_3$)$_4$] ($\gamma' = 9 \times 10^{-29}$ esu) [22] and [Et$_4$ N)$_3$[WOS_3(CuI)(μ_2-I)] ($\gamma' = 2.8 \times 10^{-29}$ esu) [35], and larger than that of C_{60} [39], but smaller than those of other cluster compounds. Hou and his co-workers deemed that 1-D chain polymers have self-defocusing behavior [40], but **3** has a self-focusing effect.

4. Conclusion

We reported three copper(II) Schiff base complexes. The secondary ligands play a crucial role in determining the molecular structures of **1–3**. All three compounds show the third-order NLO absorptive effect. Compound **3** has a positive sign for the refractive nonlinearity and gives rise to self-focusing behavior. The $|\gamma'|$ values of **1–3** are 7.6×10^{-30}, 8.2×10^{-29}, and 3.52×10^{-29} esu, smaller than those of some cluster compounds, but larger than that of C_{60}. These complexes will be good candidates for NLO materials.

Supplementary material

Crystallographic data for the structures reported in this article in the form of CIF files have been deposited with the Cambridge Crystallographic Data Center as supplementary publication Nos. 1011461, 1011462, and 1011463 for **1–3**, respectively. Copy of the data can be obtained free of charge via http://www.ccdc.cam.ac.uk/conts/retrieving.html or from CCDC, 12 Union Road, Cambridge CB2 IEZ, UK (Fax: +44 1223 336 033; Email: deposit@ccdc.cam.ac.uk).

Funding

The work was financially supported by Natural Science Fund Project of Education Department of Henan Province [grant number 13A150293]; [grant number 14A150023].

References

[1] X.H. Bu, M. Du, L. Zhang, D.Z. Liao, J.K. Tang, R.H. Zhang. *Dalton Trans.*, 593 (2001).
[2] S. Banerjee, M. Nandy, S. Sen, S. Mandal, G.M. Rosair, A.M.Z. Slawin, C.J. Gómez-García, J.M. Clemente-Juan, E. Zangrando, N. Guidolin, S. Mitra. *Dalton Trans.*, 1652 (2011).
[3] R.M. Mannar, A. Shalu, B. Cerstin, E. Martin, R. Dieter. *Dalton Trans.*, 537 (2005).
[4] E.I. Solomon, R.K. Szilagyi, S. DeBeer George, L. Basumallick. *Chem. Rev.*, **104**, 419 (2004).
[5] S. Leininger, B. Olenyuk, P.J. Stang. *Chem. Rev.*, **100**, 853 (2000).
[6] X.Y. Chen, S.Z. Zhan, C.J. Hu, Q.J. Meng, Y.J. Liu. *Dalton Trans.*, 245 (1997).
[7] R. Butcher, L. Hick, R. Kanitz, K. Maxwell, G. Mockler, C. Szczepina. *J. Coord. Chem.*, **67**, 684 (2014).
[8] V.A. Joseph, M.V. Komal, H.P. Jignesh, K.G. Vivek, R.N. Jadeja. *J. Coord. Chem.*, **66**, 1094 (2013).
[9] S. Thalamuthu, B. Annaraj, S. Vasudevan, S. Sengupta, M.A. Neelakantan. *J. Coord. Chem.*, **66**, 1805 (2013).
[10] K.R. Pothiraj, T. Baskaran, N. Raman. *J. Coord. Chem.*, **65**, 2110 (2012).
[11] R. Takjoo, J.T. Mague, A. Akbari, S.Y. Ebrahimipour. *J. Coord. Chem.*, **66**, 2852 (2013).
[12] C. Vadapalli, A. Ramachandran, T.S.A. Gurusamy, K. Venkatasubbaiah, Z. Stefano, F.B. Jamie, S. Alexander, J.B. Raymond, K. Paul. *Inorg. Chem.*, **42**, 5989 (2003).
[13] C. Vadapalli, A. Ramachandran, Z. Stefano, F.B. Jamie, S. Alexander. *Inorg. Chem.*, **44**, 4608 (2005).
[14] Q.F. Zhang, F.L. Jiang, Y.G. Huang, M.Y. Wu, M.C. Hong. *Cryst. Growth Des.*, **9**, 28 (2009).
[15] L.M. Wu, H.B. Teng, X.C. Feng, X.B. Ke, Q.F. Zhu, J.T. Su, W.J. Xu, X.M. Hu. *Cryst. Growth Des.*, **7**, 1337 (2007).
[16] D. Sadhukhan, A. Ray, G. Pilet, C. Rizzoli, G.M. Rosair, C.J. Gómez-García, S. Signorella, S. Bellú, S. Mitra. *Inorg. Chem.*, **50**, 8326 (2011).
[17] L.M. Wu, G.F. Qiu, H.B. Teng, Q.F. Zhu, S.C. Liang, X.M. Hu. *Inorg. Chim. Acta*, **360**, 3069 (2007).
[18] R. Luca, F. Alessandra, P. Roberta, R. Jan, P. Alessandro. *Dalton Trans.*, **40**, 3381 (2011).
[19] D.S. Chemla, J. Zyss. *Nonlinear Optical Properties of Organic Molecules and Crystal*, Academic, Orlando, FL (1987).
[20] H. Huang. *Optical Nonlinearities and Instabilities in Semiconductors*, Academic Press, Boston, MA (1988).
[21] H.W. Hou, H. Ghee Ang, S. Gek Ang, Y.T. Fan, M.K.W. Low, W. Ji, Y. Wang Lee. *Phys. Chem. Chem. Phys.*, **1**, 3145 (1999).

[22] S. Shi, H.W. Hou, X.Q. Xin. *J. Phys. Chem.*, **99**, 4050 (1995).
[23] H.W. Hou, D.L. Long, X.Q. Xin, X.X. Huang, B.S. Kang, P. Ge, W. Ji, S. Shi. *Inorg. Chem.*, **35**, 5363 (1996).
[24] Y.Y. Niu, T.N. Chen, S.X. Liu, Y.L. Song, Y.X. Wang, Z.L. Xue, X.Q. Xin. *Dalton Trans.*, 1980 (2002).
[25] A. Houlton, N. Jassim, R.M.G. Roberts, J. Silver, P. McArdle, T. Higgins. *Dalton Trans.*, 2235 (1992).
[26] J. Silver, J.R. Miller, A. Houlton, M.T. Ahmet. *J. Chem. Soc., Dalton Trans.*, 3355 (1994).
[27] S.K. Pal, A. Krishnan, P.K. Das, A.G. Samuelson. *J. Organomet. Chem.*, **604**, 248 (2000).
[28] G.M. Sheldrick. *Acta Cryst.*, **64**, 112 (2008).
[29] N. Zhao. *Acta Cryst.*, **C69**, 348 (2013).
[30] M.F. Iskander, T.E. Khalil, W. Haase, S. Foro, H.J. Lindner. *J. Coord. Chem.*, **58**, 111 (2005).
[31] A. Roth, A. Buchholz, W. Plass. *Z. Anorg. Allg. Chem.*, **633**, 383 (2007).
[32] X.Y. Chen, S.H. Zhan, Q.J. Meng. *Transition Met. Chem.*, **21**, 345 (1996).
[33] M. Sheik-Bahae, A.A. Said, T.H. Wei, D.J. Hagan, E.W. Van Stryland. *IEEE J. Quantum Electron.*, **26**, 760 (1990).
[34] M. Sheik-bahae, A.A. Said, E.W. Van Stryland. *Opt. Lett.*, **14**, 955 (1989).
[35] H.W. Hou, B. Liang, X.Q. Xin, K.B. Yu, P. Ge, W. Ji, S. Shi. *Dalton Trans.*, **92**, 2343 (1996).
[36] B. Wu, W.H. Zhang, H.X. Li, Z.G. Ren, J.P. Lang, Y. Zhang, Y.L. Song. *J. Mol. Struct.*, **829**, 128 (2007).
[37] Z.G. Ren, H.X. Li, L.L. Li, Y. Zhang, J.P. Lang, J.Y. Yang, Y.L. Song. *J. Organomet. Chem.*, **692**, 2205 (2007).
[38] S. Shi, W. Ji, W. Xie, T.C. Chong, H.C. Zeng, J.P. Lang, X.Q. Xin. *Mater. Chem. Phys.*, **39**, 298 (1995).
[39] Y. Wang, L.T. Cheng. *J. Phys. Chem.*, **96**, 1530 (1992).
[40] H.W. Hou, X.R. Meng, Y.L. Song, Y.T. Fan, Y. Zhu, H.J. Lu, C.X. Du, W.H. Shao. *Inorg. Chem.*, **41**, 4068 (2002).